25th ABCM International Congress of Mechanical Engineering
October 20-25, 2019, Uberlândia, MG, Brazil

COB-2019- 1141
AERODYNAMIC EFFECTS OF ASYMMETRICAL LEADING EDGE PROTUBERANCES ON A RECTANGULAR WING

Juan Antonio Flores Mezarina
Daniel Garcia Ribeiro
Pedro David Bravo-Mosquera
Hernan Dario Cerón-Muñoz
da Escola de Engenharia de São Carlos – EESC / USP
Programa de Pós-Graduação em Engenaria Mecânica
Av. Trabalhador São-Carlense, 400. Caixa Postal 359. CEP 13566-590 – São Carlos, SP – Brazil
juan.flores@usp.br
ribeiro.danielg@usp.br
pdbravom@usp.br
hernan@sc.usp.br

Abstract. *The phenomenon produced by symmetrical protuberances, or tubercles, on the leading edge of a wing, also known as Wavy Leading Edge, has been widely studied on the last decades. They delay the stall angle, improve the performance on stall and post stall regime and reduce the span-wise flow by counter-rotating vortices generation. Recent WLE studies carried in swept wings showed significant increment of lift and reduction of the wing tip vortex' strength. Although swept wings turn protuberances asymmetrical along the wingspan, this asymmetry hasn't been parameterized and is only dependent to the sweep angle. The aim of this study is to introduce an asymmetry parameter, independent of the sweep angle, and to study its effects for different asymmetry configurations on a rectangular wing. Through wind tunnel measures and visualization tests, it was found that asymmetrical protuberances may have a great effect over cross-flow and induced drag.*

Keywords: *Asymmetrical leading-edge protuberances, asymmetrical WLE, cross-flow reduction*

1. INTRODUCTION

Humpback whales' high maneuverability has inspired numerous studies. It was found that the protuberances, or tubercles, on the leading edge of their pectoral flippers act as a passive control device (Fish and Battle, 1995) (Watts and Fish, 2001). Much of the current literature pays particular attention to their stall and post-stall benefits. Miklosovic et al. (2004) reported that the stall angle of an idealized humpback whale flipper with leading-edge protuberances is delayed by approximately 40%. Lift and drag present practically no variation before the stall angle; but along the angles of delayed stall, lift presents significant increase and drag is reduced up to 32%. Additionally, stall turns less abrupt. Cai et al. (2013) evaluated numerically the effect of leading edge protuberances on the stall characteristics. They concluded that for both, static and dynamic stall, an airfoil with protuberances has more stable characteristics. Leading edge protuberances cause high consistency of flow. Contrary to Miklosovic et al. (2004), they showed that lift at pre-stall regime and maximum lift are degraded.

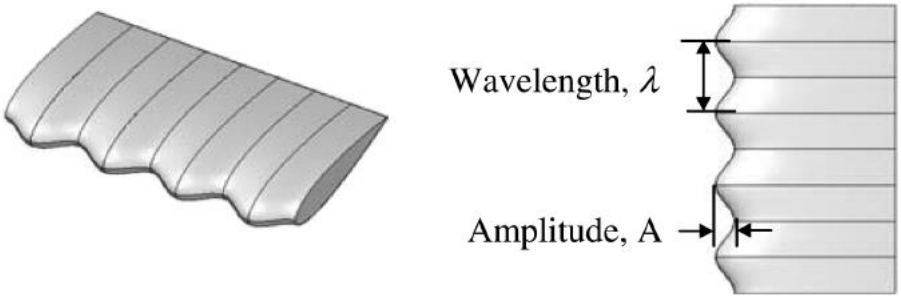

Figure 1. Goberning parameters of leading-edge protuberances, adapted from Jhari (2007)

Both parameters to generate the protuberances, amplitude and wavelength (λ), see Fig. 1, were first varied by Johari et al. (2007) to examine its variation effect. It was concluded that, in contrast to wavelength, amplitude variation's effect is significant on the resulting forces and moments. On the other hand, Hansen, Kelso and Dally (2011) realized that by decreasing amplitude, lift and drag perform in a similar manner to the base model but, by increasing amplitude, lift performance is increased in the post-stall regime but degraded in the pre-stall regime. Decrease of wavelength up to a certain limit benefits the maximum lift, stall transition and, even drag in a slight manner.

Watts and Fish (2001) compared by CFD simulations the pressure profile on the suction side of a base smooth leading edge wing and a modified wing with protuberances. Pressure over the base wing is uniform along the span while varies along the chord. In contrast, pressure over the modified wing is greater behind the protuberances' peaks than behind the troughs. Dropkin *et al*. (2012) illustrated in more detail the difference of pressure profiles at different angles of attack (α), see Fig. 2. For low α, pressure over the base model remains uniform along the span while varies in the chord wise. Small local stall cells appear and grow towards the leading edge as α increases. Near the stall angle, the stall cells have grown, merged and approached to the leading edge. When stall occurs, flow separates right after the leading edge and decreases dramatically lift. On the other hand, pressure profile of the WLE model corresponds to the leading edge geometry. At low α, low pressure capsules appear behind every trough along the span. Local stall cells appear at smaller α than the base model behind the low pressure capsules. When α approaches the base stall angle, trough capsules increase and decrease alternately between successive troughs. This alternated pattern is accentuated with increase of α, capsules enlarge but get thinner. Some of them eventually vanish and the ones left merge. For α beyond base model stall angle, there are few enlarged low pressure capsules remaining.

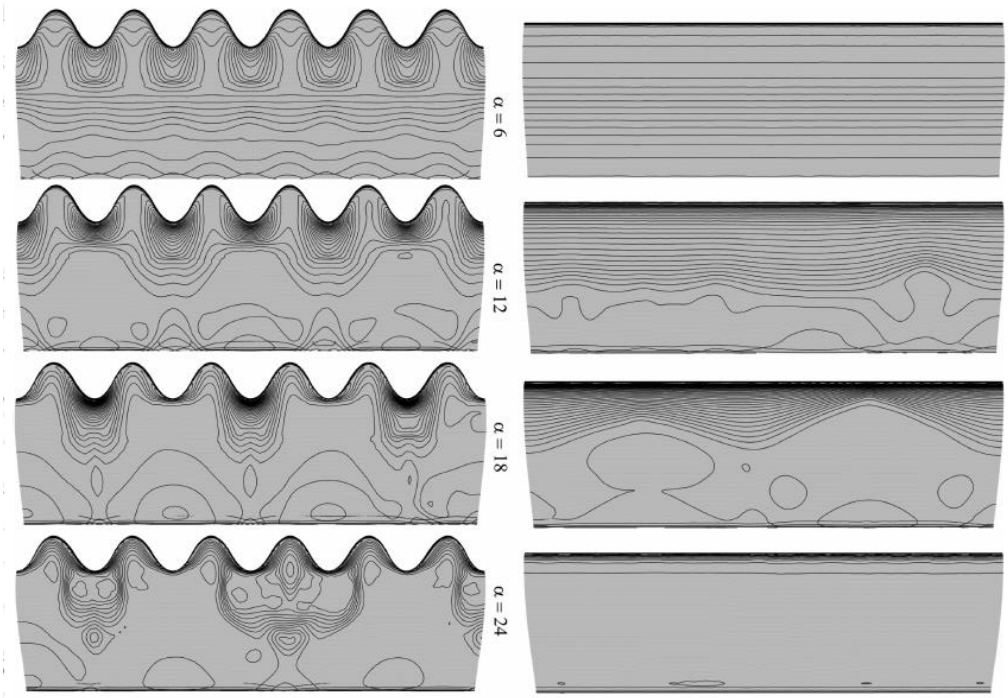

Figure 2. Pressure contours comparison between the base and modified wings, adapted from Dropkin *et al*. (2012)

Several CFD analysis and visualization studies have focused their attention to better understanding the flow dynamics around leading-edge protuberances. Dye visualization tests performed by Custodio (2007) illustrated the near surface flow dynamics over the suction side of a wing with leading edge protuberances (Fig. 3). Fluids' tendency to move from high to low pressure areas generate a span-wise component from the peaks to the troughs. This span component is almost insignificant at α=0 but increases as α does and generates symmetrical counter-rotating streamwise vortices in each side of the peaks. Carreira Pedro and Kobayashi (2008) stated that these counter rotating vortices perform as passive wing fences that reduce the intensity of span-wise flow. In comparison with the base model; boundary layer separation is delayed after the protuberances due to the non-uniform behavior of the fluid after each protuberance (Nierop, Alben and Brenner, 2008). Boundary layer separation occurs before in the troughs while flow remains attached behind the peaks, as illustrated by large-eddy simulations (Pérez-Torró and Kim, 2017).

Protuberances vortices generation was further studied in swept wings (Bolzon, Kelso and Arjomandi, 2016). Swept angle causes proportional deformation of the protuberances, turning them asymmetrical in the span-wise. This asymmetry causes the counter-rotating vortices to have asymmetrical intensity, which enhances the fence effect

previously stated. Vorticity contours showed that local circulation is enhanced behind the waves. This may not help reducing drag but, counteracts the flow in the span-wise and the accumulation of vorticity to the wingtip. As result, the tip vortex strength decreased dramatically. Wei, Lian and Zhong (2018) used aerodynamic tests to evaluate the effect of protuberances in the hydrodynamic performance of tapered swept wings. They found that although there is a slight increase of drag near the stall angle, overall lift is enhanced at all tested angles; therefore, performance is also enhanced. De Paula et al. (2018) reported that the protuberances' efficiency varies with the sweep angle and taper ratio, which have direct effect on the protuberances' asymmetry.

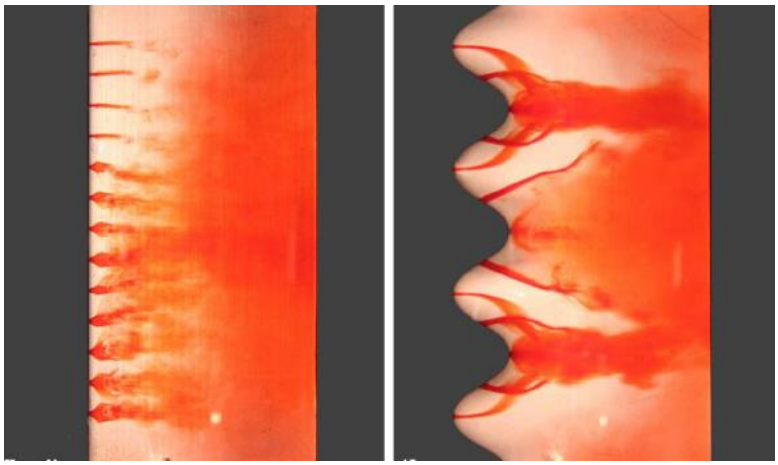

Figure 3. Dye visualization test, adapted from Custodio (2007)

However, protuberances' asymmetry previously studied was only the result of the swept angle; there is not a specific parameter or method that controls this asymmetry. In this study, we present a method to control protuberances' asymmetry for either swept or straight wings. The effect of asymmetrical protuberances was quantified and qualified by wind tunnel measurements and flow visualization tests.

2. EXPERIMENTAL SETUP

2.1 Asymmetry parameterization

The asymmetry parameter (established as d) was set as a function of the peak's position along the wavelength:

Table 1. Asymmetry parameter.

Wavelength	Peak's Position	$d = \frac{peak's\ position}{wavelength}$
2π	π (symmetry)	$\pi/2\pi = 0.50$
	0.8π	$0.8\pi/2\pi = 0.40$
	0.6π	$0.6\pi/2\pi = 0.30$
	0.4π	$0.4\pi/2\pi = 0.20$

In most of the previous studies protuberances have been created by superimposing sinusoidal functions to the base model, this creates continuous symmetrical protuberances along the spanwise. Eq. (1) shows Miklosovic et al. (2007) equation.

$$\Delta x_{LE} = 0.125(1 - 0.001y^2)\sin(0.57y^{1.5} - 0.4)\,[\tanh(y - 7) + 1] \tag{1}$$

In this study, the asymmetry parameter was implemented in a function to create the asymmetrical protuberances. The function has the format:

$$x_{LE} = A\,cos(By + Cy^{4.5}) \tag{2}$$

Where A depends on the amplitude. B and C, depend on the wavelength (λ), asymmetry factor (d) and wing's chord.

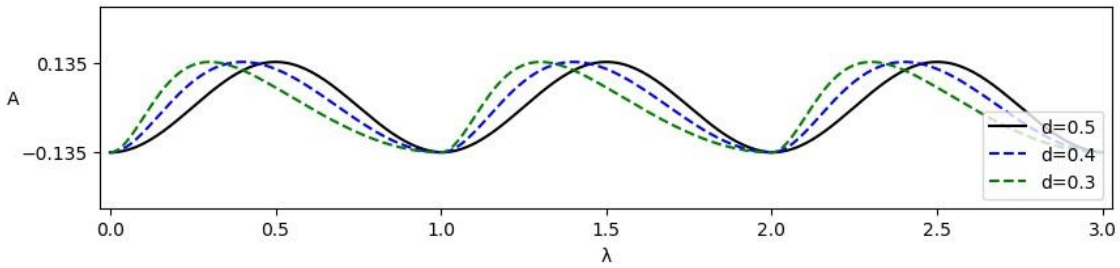

Figure 4. Symmetrical (black line) and asymmetrical (blue and green lines) protuberances.

2.2 Wing models

Test models were projected on a base of the NACA 0021 airfoil. According to Hansen et al. (2011), leading-edge tubercles best perform at wave length approximately 21% of the chord, and at amplitude/wavelength relationship (A /λ) of 0.27. Test models' amplitude and wavelength were set at 22% and 6% of the chord respectively.

The wings were projected straight, without swept angle or taper ratio. Chord was set in 15cm and span in 60cm, as shown in Fig. 5.

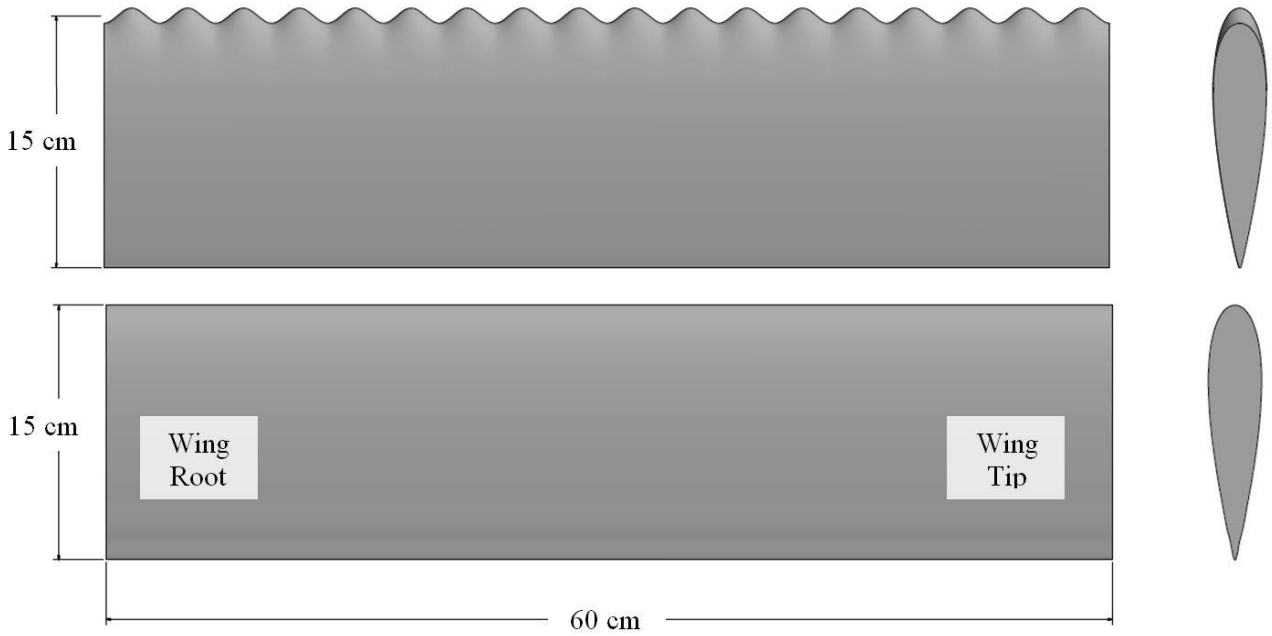

Figure 5. Wings dimensions

Eight different configurations, shown in Table 2, were printed in Polylactic Acide (PLA). Their nomenclature corresponds to the base airfoil (NACA0021), and the asymmetry parameter (Except for the Smooth model).

Table 2 – Built models and their nomenclature.

Label	d	Asymmetry Detail	Label	d	Asymmetry Detail
N21Smth	-		N21d50	0.50	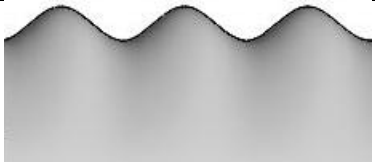

N21d40	0.40	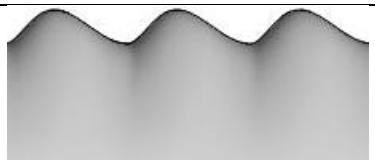	N21d60	0.60	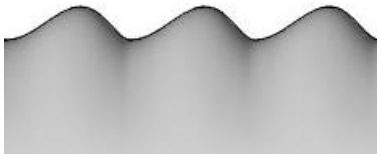
N21d30	0.30	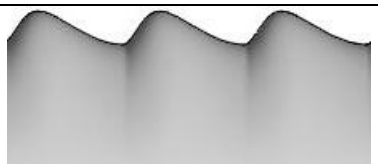	N21d70	0.70	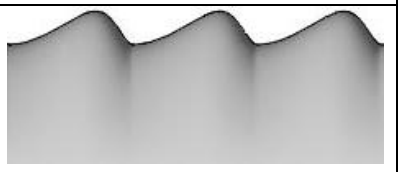
N21d20	0.20	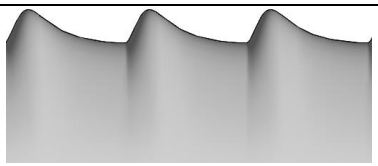	N21d80	0.80	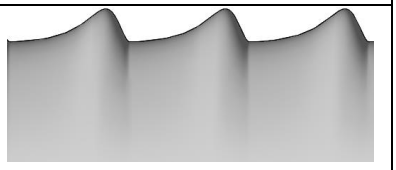

2.3 Wind tunnel tests

The wind tunnel testing and flow visualization tests were carried at the facilities of the São Carlos School of Engineering – University of São Paulo (EESC-USP). The tests were carried in a closed test section of 0.8 x 1.05 m. The wind speed was set at 25.5 m/s and Re ≈ 2.5×10^5. Lift and drag were measured with uncertainty of ± 0.01N on an aerodynamic balance assembled to the test camera. A micro manometer of uncertainty ± 0.1Pa was used to measure dynamic pressure. Uncertainty of both wings' span and chord was ± 0.001m.

For visualization, it was used a mixture of vegetable oil and fine pigment over the wings' surface, the surface oil-flow technique. This allowed observing all the vortices generated at the leading edge by the protuberances and the behavior of flow along the chord.

3. RESULTS

3.1 Wind tunnel measurements

The results were divided in two comparative groups: a) Asymmetrical peaks toward the wing root, b) Asymmetrical peaks toward the wing tip. Lift and drag coefficients are illustrated in Figures 6 and 7. For the first group (a), it is evidenced that the asymmetrical protuberances enhanced the 3D effects on the wind. The lift slope in pre-stall and maximum CL decreased while drag slightly increased. The second group (b) showed similar behavior to the symmetrical protuberances.

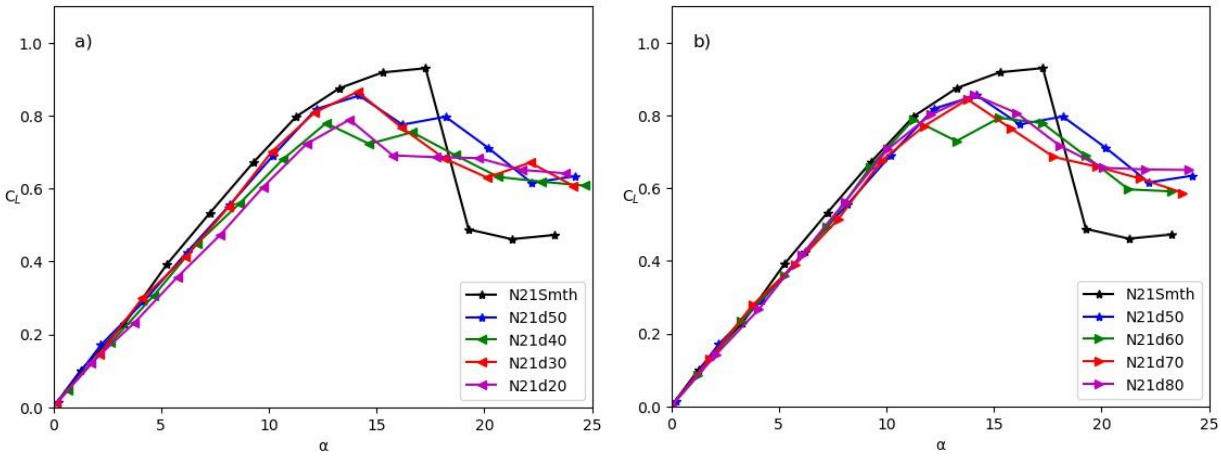

Figure 6. CL vs Alpha.

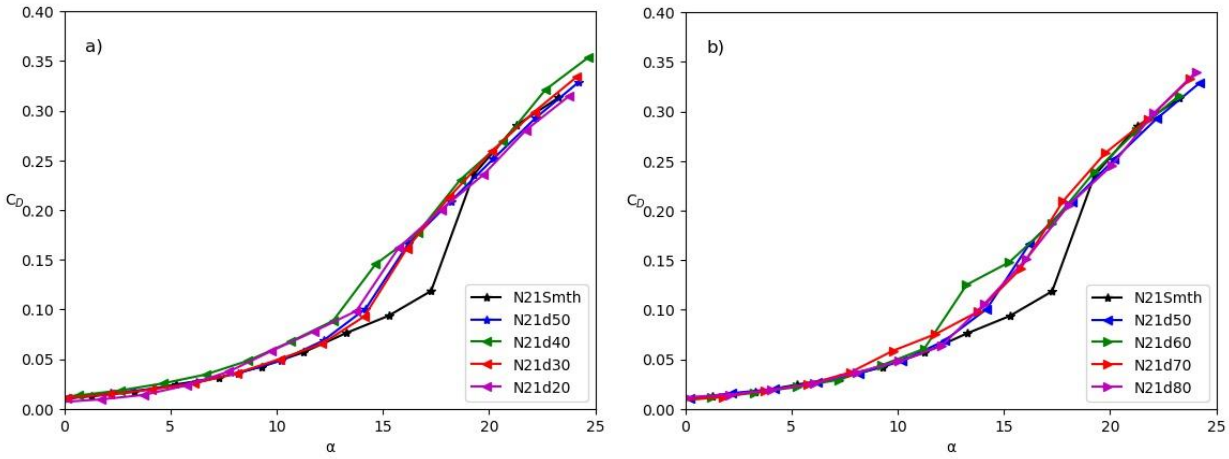

Figure 7. CD vs Alpha.

Total drag (C_D) is the sum of parasite(C_{D_0}) and induced drag as shown in equations 3 and 4; where AR is the aspect ratio (Eq. 5), e_0 is the aerodynamic efficiency coefficient, b the span length and S the wing's area:

$$C_D = C_{D_0} + kC_L^2 \tag{3}$$

$$C_D = C_{D_0} + \frac{C_L^2}{\pi \cdot AR \cdot e_0} \tag{4}$$

$$AR = \frac{b^2}{S} \tag{5}$$

AR is practically constant for all the models. Figure 8 shows that there is no significant increase on parasite drag. Therefore, total drag increase corresponds to induced drag increase. As it depends on C_L^2, any drag increase for the same C_L^2 value indicates decrease of the Oswald coefficient (span efficiency) e_0. It is remarkable the difference between the asymmetrical groups. Asymmetrical models in a) present significant increment of induced drag, while the ones in b) present minor increase of induced drag.

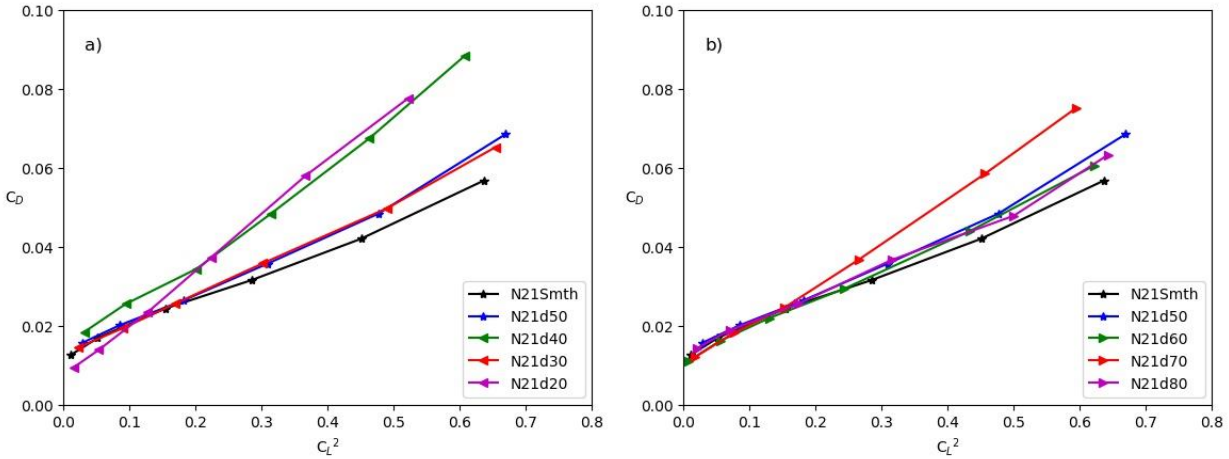

Figure 8. CD vs CL^2.

Figures 9 to 11 illustrate the models' aerodynamic efficiency. When compared to the smooth leading edge or to the model with symmetrical protuberances, asymmetrical models in a) seem to significantly degrade their aerodynamic performance in the pre-stall regime. It is possible that these asymmetrical configurations (peaks toward the wing root) enhance the flow separation that starts at the wing root.

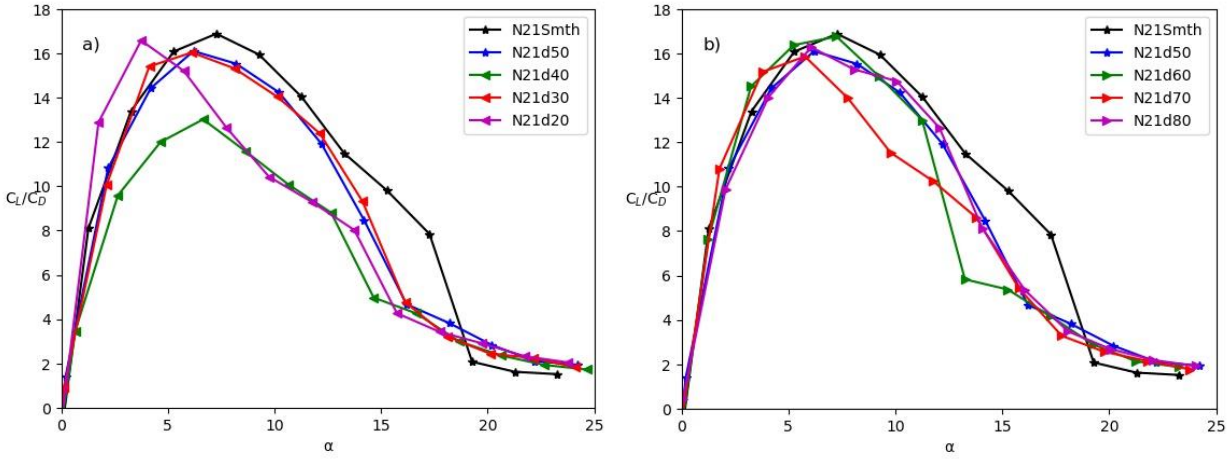

Figure 9. CL/CD vs Alpha.

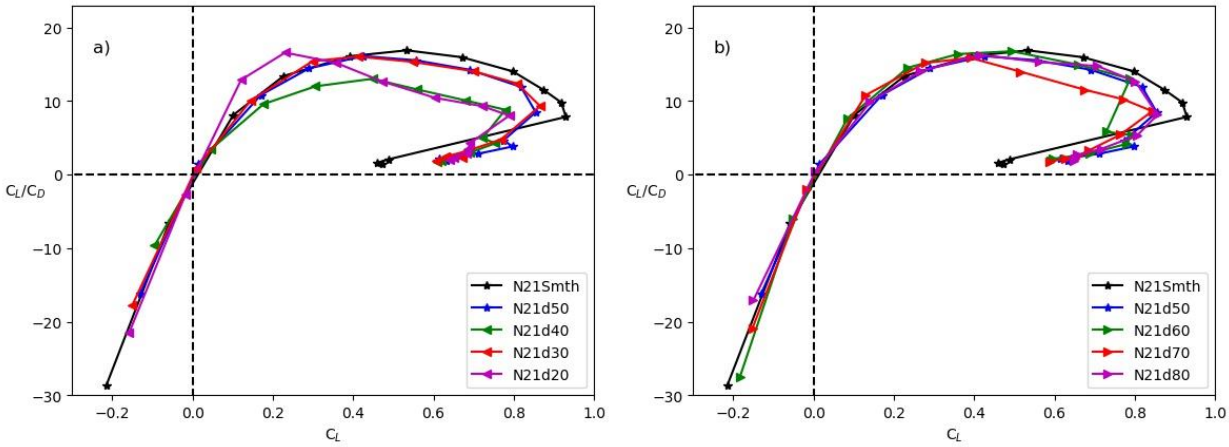

Figure 10. CL/CD vs CL.

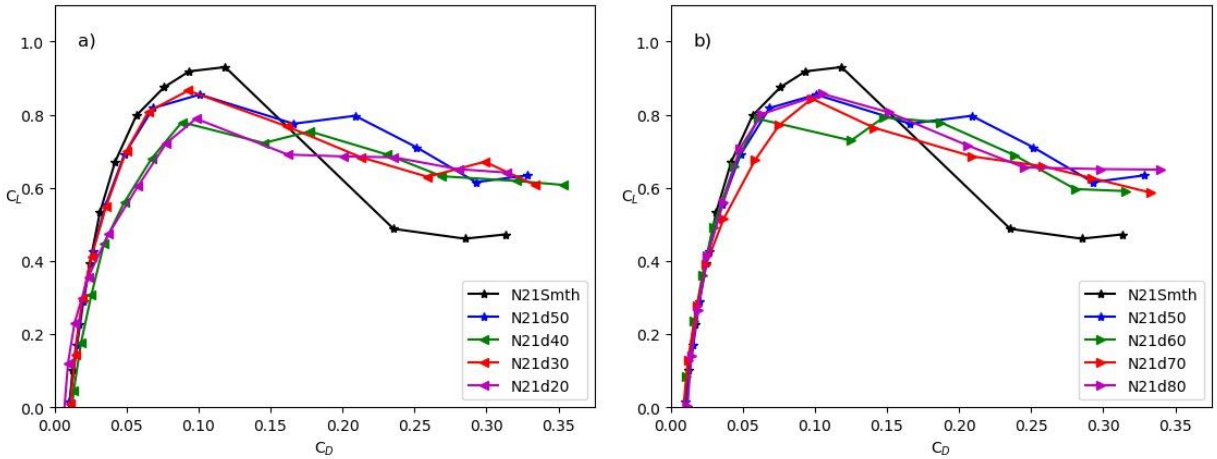

Figure 11. CL vs CD.

3.2 Flow visualization

Pressure contours obtained by CFD analyze showed that low pressure capsules and pressure gradients depend on the protuberances' shape, see Fig. 12. Asymmetrical protuberances cause the low pressure capsules to turn asymmetrical as well. Hence, unbalanced pressure gradients generate unbalanced counter-rotating stream-wise vortices. The unbalance direction depends on the peaks location.

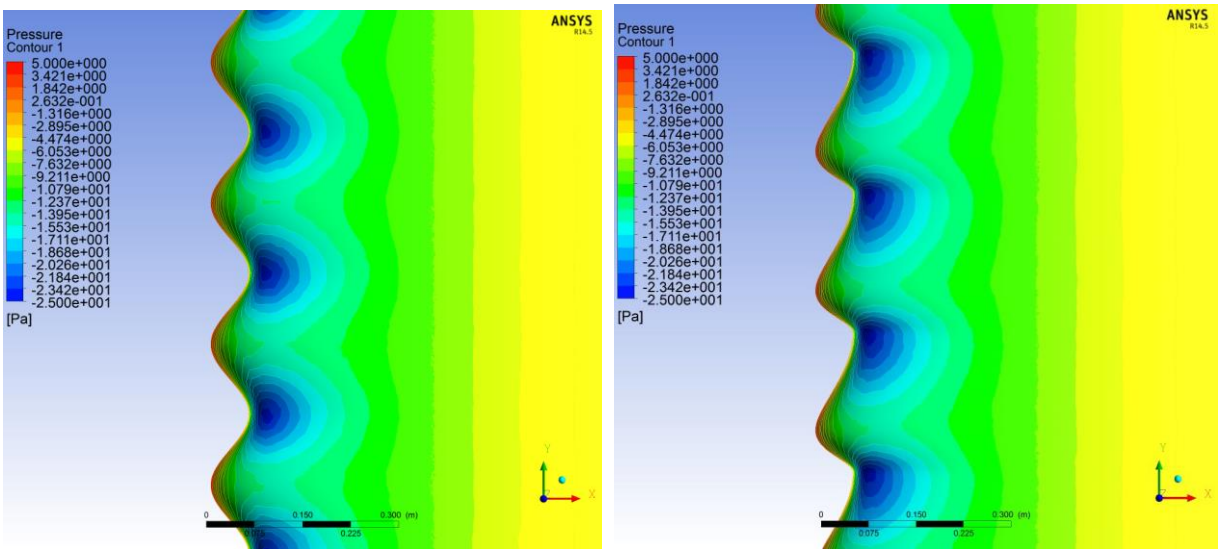

Figure 12. Pressure contours obtained by CFD analyze.

Flow visualization test carried on the N21d20 and N21d50 models showed coherence to the CFD analyze. When compared, the difference of vortices' format is clear.

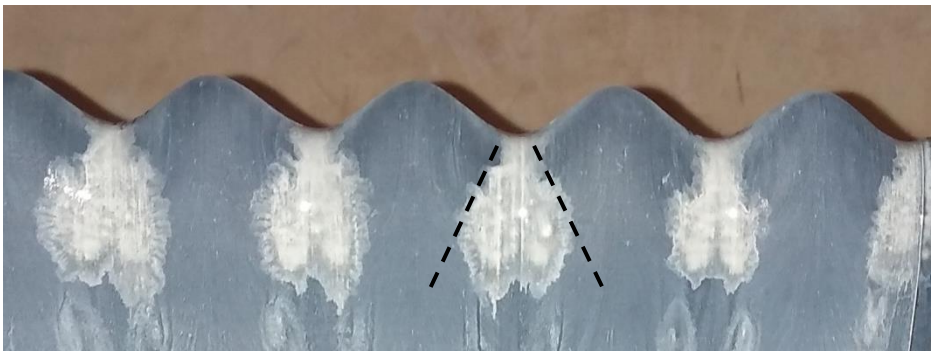
Figure 13. Flow visualization of the vortices at the troughs of the symmetrical model (N21d50)

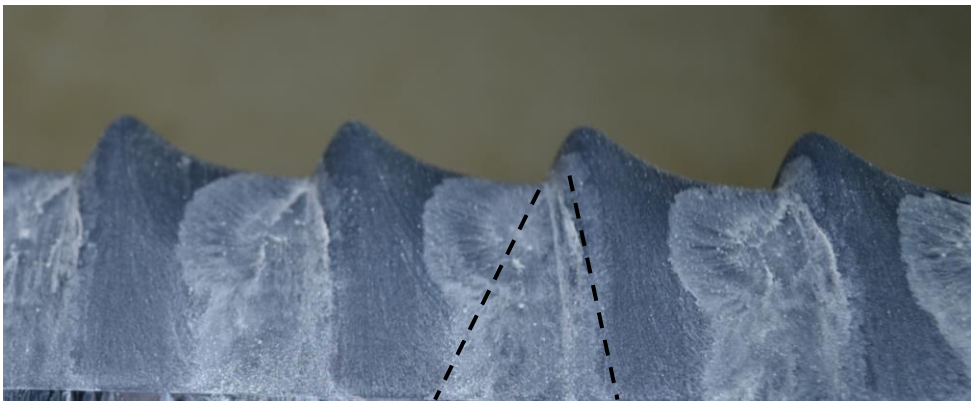
Figure 14. Flow visualization of the vortices at the troughs of the model N21d20.

4. CONCLUSIONS

In this study, asymmetry was introduced as a new parameter for leading edge protuberances. The asymmetry factor was established as the protuberance's peak position along its wavelength. A set of eight wings was built to carry wind tunnel measurement and flow visualization tests. As a preliminary study, the aim was to compare aerodynamic characteristics of asymmetrical and symmetrical leading edge protuberances. The simple straight wing geometry was chosen as start point to expand the study of asymmetrical protuberances. Most of the asymmetrical models showed slight degradation of the aerodynamic performance of the wings. Nevertheless, flow visualization tests and CFD

pressure contours indicate that asymmetry may have a relevant effect on cross-flow. The orientation of asymmetry may enhance or diminish the cross-flow intensity and consequently induced drag.

5. ACKNOWLEDGEMENTS

The authors thank financial support of CAPES (Coordenação de Aperfeiçoamento de Pessoal de Nível Superior) - Finance Code 001 and CNPq (Conselho Nacional de Desenvolvimento Científico e Tecnológico).

6. REFERENCES

Fish,F. E. and Battle, J. M., 1995. "Hydrodynamic Design of the Humpback Whale Flipper". *Journal of Morphology*, Vol. 225, No. 1, pp 51-60

Watts, p. and Fish, F. E., 2001. "The Influence of Passive, Leading Edge Tubercles on Wing Performance". *In Proc. Twelfth Intl. Symp. Unmanned Untethered Submers. Technol*. Durham New Hampshire: Auton. Undersea Syst. Inst.

Miklosovic, D. S., Murray, M. M., Howle, L. E., and Fish, F. E., 2004. "Leading-edge tubercles delay stall on humpback whale (Megaptera novaeangliae) flippers". *Physics of fluids*, Vol 16, No. 5, pp. L39-L42.

Cai, C., Zuo, Z., Liu, S., Wu, Y., Wang, F., 2013. "Numerical evaluations of the effect of leading-edge protuberances on the static and dynamic stall characteristics of an airfoil." IOP Conference Series: Materials Science and Engineering; Vol. 52, No. 5, pp. 022006.

Johari, H., Henoch, C. W., Custodio, D., and Levshin, A., 2007. "Effects of leading-edge protuberances on airfoil performance". *AIAA Journal*, Vol. 45, No. 11, pp. 2634-2642.

Hansen, K. L., Kelso, R. M., and Dally, B. B., 2011. "Performance variations of leading-edge tubercles for distinct airfoil profiles". *AIAA Journal*, Vol. 49, No. 1, pp. 185-194.

Dropkin, A., Custodio, D., Henoch, C., and Johari, H., 2012. "Computation of flow field around an airfoil with leading-edgeprotuberances", *Journal of Aircraft*, Vol. 49, No. 5, pp. 1345-1355.

Carreira Pedro, H., and Kobayashi, M. ,2008. "Numerical study of stall delay on humpback whale flippers". In *46th AIAA aerospace sciences meeting and exhibit.* pp. 584.

Custodio, D. S., 2007. *The Effect of Humpback Whale-like Protuberances on Hydrofoil Performance.* Master theses, Worcester Polytechnic Institute, Massachusetts, USA.

Van Nierop, E. A., Alben, S., and Brenner, M. P., 2008. "How bumps on whale flippers delay stall: an aerodynamic model". *Physical review letters*, Vol. 100, No. 5, pp. 054502.

Pérez-Torró, R., and Kim, J. W., 2017. "A large-eddy simulation on a deep-stalled aerofoil with a wavy leading edge". *Journal of Fluid Mechanics*, Vol. 813, pp.23-52.

Bolzon, M. D., Kelso, R. M., and Arjomandi, M., 2016. "Formation of vortices on a tubercled wing, and their effects on drag". *Aerospace Science and Technology*, Vol. 56, pp. 46-55.

Wei, Z., Lian, L., and Zhong, Y., 2018. "Enhancing the hydrodynamic performance of a tapered swept-back wing through leading-edgetubercles", *Experiments in Fluids*, Vol. 59, No. 6, pp. 103.

de Paula, A. A., Rios Cruz, A. A., Ferreira, P. H., Kleine, V. G., and da Silva, R. G., 2018. "Swept wing effects on Wavy Leading Edge Phenomena". In *2018 Flow Control Conference.* pp. 4253.

7. RESPONSIBILITY NOTICE

The authors are the only responsible for the printed material included in this paper.